VCAM-1 directed immunoliposomes selectively target tumor vasculature *in vivo*

Sara Gosk [a,*], Torben Moos [b], Claudia Gottstein [c,1], Gerd Bendas [a,1]

[a] *University of Bonn, Department of Pharmacy, An der Immenburg 4, 53121 Bonn, Germany*
[b] *Department of Medical Anatomy, The Panum Institute, University of Copenhagen, Copenhagen, Denmark*
[c] *University of California Santa Barbara, Department of Chemical Engineering, California NanoSystems Institute, Santa Barbara, CA 93106-5080, USA*

Abstract

Targeting the tumor vasculature and selectively modifying endothelial functions is an attractive anti-tumor strategy. We prepared polyethyleneglycol modified immunoliposomes (IL) directed against vascular cell adhesion molecule 1 (VCAM-1), a surface receptor over-expressed on tumor vessels, and investigated the liposomal targetability *in vitro* and *in vivo*. *In vitro*, anti-VCAM-1 liposomes displayed specific binding to activated endothelial cells under static conditions, as well as under simulated blood flow conditions. The *in vivo* targeting of IL was analysed in mice bearing human Colo 677 tumor xenografts 30 min and 24 h post i.v. injection. Whereas biodistribution studies using [3H]-labelled liposomes displayed only marginal higher tumor accumulation of VCAM-1 targeted versus unspecific ILs, fluorescence microscopy evaluation revealed that their localisations within tumors differed strongly. VCAM-1 targeted ILs accumulated in tumor vessels with increasing intensities from 30 min to 24 h, while control ILs accumulated in the tumor tissue by passive diffusion. ILs that accumulated in non-affected organs, mainly liver and spleen, primarily co-localised with macrophages. This is the first morphological evidence for selective *in vivo* targeting of tumor vessels using ILs. VCAM-directed ILs are candidate drug delivery systems for therapeutic anti-cancer approaches designed to alter endothelial function.
© 2007 Elsevier B.V. All rights reserved.

Keywords: Immunoliposome; Tumor; Vascular targeting; VCAM-1; Tumor xenograft model

1. Introduction

Specific delivery of therapeutic agents incorporated into nanoparticles, such as liposomes, to endothelial cells is an attractive strategy for modifying vascular function in various pathological states, e.g. cancer and inflammation. Accordingly, there is an increasing interest in approaches that target the tumor vasculature during growth, development and metastasis and aim at either destroying existing tumor vessels, specifically occluding tumor vasculature or at interfering with the process of angiogenesis [1–3]. Vascular targeting agents bypass the need for extravasation from the bloodstream, as endothelial cells are directly accessible to i.v. administered drugs. Targeting the vasculature offers several additional advantages: 1) an ampli-fication effect, as each tumor vessel feeds a large number of tumor cells; 2) a reduced risk of acquired drug resistance because endothelial cells are genetically more stable than tumor cells [4]; 3) a broad application spectrum since tumor endothelial cell markers are shared by many different tumor types [5] and since the dependence of tumor growth on neovascularisation [6] is not tumor type specific.

Liposomes are biocompatible nanoscale drug carriers systems. Their sterical stabilisation by, e.g. incorporation of polyethyleneglycol (PEG) lipids into the bilayer mediates long circulation half-lives of about 16 h in mice or rats, and 24 h or longer in humans after i.v. administration [7]. The coupling of antibodies onto the surface of PEGylated liposomes results in immunoliposomes (ILs) and allows for specific targeting [8]. ILs have been studied extensively with respect to the antibody coupling procedure [9], sterical stabilization [10] and immunogenicity [11,12]. Several *in vitro* studies reported targeting of ILs to endothelial cells with the future goal to localise liposomes

---

to sites of inflammation or tumor vasculature. The targeted receptors in those studies included endoglin [13], vascular endothelial growth factor receptor 2 [14], intercellular adhesion molecule 1 [15], E-selectin [16,17] and vascular cell adhesion molecule 1 (VCAM-1) [18–20]. *In vivo*, ILs have been demonstrated to target to inflamed vasculature [21] or vessels in the area of myocardial infarction [22].

Several *in vivo* studies have investigated the vascular targetability of liposomes decorated with peptides. These peptides include RGD motifs binding to $\alpha_v\beta_3$ integrins [reviewed in [23], NGR motifs binding to aminopeptidase N [24], CREKA binding to fibrinogen or fibrin [25], or GPLPLR binding to membrane type-1 matrix metalloproteinase [26]. While the generally lower binding affinity of peptides compared to antibodies can be of advantage for targeting the *tumor cell* compartment [27] high affinity binding appears to be preferable for robust *tumor vascular* targeting, since ligands binding to the luminal side of blood vessels are exposed to the dynamic flow environment of the bloodstream. Multivalent avidity effects can drastically increase overall binding of particles coated with low affinity ligands; yet Zhou et al. reported that below a certain ligand density the affinity of the monovalent ligand influences the binding properties of the multivalent particle [28].

In order to generate carriers with sufficient binding affinity and selectivity, the experimental design introduced here incorporates the use of an anti-VCAM antibody as a homing device. VCAM-1 is an immunoglobulin-like transmembrane glycoprotein expressed on activated endothelial cells during inflammation and cancer [29]. VCAM-1 promotes firm cell–cell adhesion. One of its ligands is the integrin VLA-4 which is expressed on inflammatory leukocytes, on some tumor cells and also on tumor endothelial cells. The VCAM–VLA4 interaction promotes cell–cell contact between leukocytes and inflamed endothelium [30], VCAM-positive pericytes and tumor endothelium [31], proangiogenic macrophages and tumor endothelium [32], and metastatic tumor cells and tumor vasculature [33] and thus plays a role in tumor angiogenesis and metastasis. VCAM-1 expression is inducible and virtually absent on normal human vasculature [34]. Non-vascular cells with VCAM-1 expression include bone marrow cells, follicular dendritic cells, fibroblasts, and epithelial cells in the kidney [35,36]. Several diseases are associated with VCAM-1 expression on the vascular endothelium, such as atherosclerosis, inflammatory diseases and autoimmune diseases [37]. In cancer, the robust vascular VCAM-1 expression has been observed in leukemias and lymphomas, such as Hodgkin's disease and B-CLL, and to varying extents also in a variety of solid tumors such as lung cancer, breast cancer, melanoma, renal cell carcinoma, gastric cancer and nephroblastoma [reviewed in [38]]. Upon ligand binding, VCAM-1 is internalised via a clathrin dependent pathway with a half life of 15 min [39].

The biodistribution of sterically stabilized liposomes after systemic administration has been studied extensively [reviewed in [7]]. Although a dominant fraction of liposomes is taken up by organs attributed to elimination through the reticuloendothelial system (RES), especially liver and spleen, the long systemic circulation time of PEGylated liposomes permits accumulation of liposomes in non-RES sites, such as inflammatory or tumor tissues [40,41].

In this study, we investigated whether PEGylated immunoliposomes directed against a tumor vascular surface receptor would selectively bind activated endothelial cells *in vitro* and home to tumors *in vivo*. In addition, the cellular *in vivo* distribution of VCAM-targeted ILs within target and non-target tissues was assessed. To our knowledge this is the first report to demonstrate morphological evidence of IL targeting to tumor vasculature *in vivo*. Our findings suggest VCAM-directed ILs as promising carriers for anti-tumor therapeutics at the endothelial level.

2. Materials and methods

2.1. Reagents

Reagents were obtained from the following sources: soy phosphatidyl choline (SPC) was kindly donated by Lipoid AG Ludwigshafen (Germany), polyethylenglycol-phosphatidylethanolamine (PEG-PE) was purchased from Avanti Polar Lipids (Alabaster, USA). Cyanuric chloride, cholesterol (Chol), 1-ethyl-3-(3-dimethylaminopropyl) carbodiimide (EDC), *N,N*-diisopropylethylamine, 3,3′-Dioctadecyloxacarbocyanine perchlorate (DiO) and recombinant murine tumor necrosis factor-α (TNF-α), Folin–Ciocalteus phenol were from Sigma-Aldrich (Deisenhofen, Germany). The membrane anchor, cyanur-PEG-PE, for antibody coupling was synthesized by our group as previously described [42]. Antibodies used in this study were as follows: rat anti-mouse VCAM-1 (clone MK271), rat anti-mouse CD31 (clone 390) and rat anti-mouse Meca32 antigen (clone Meca32) were purified from hybridoma cell supernatant (see Section 2.2) using rat anti-mouse-IgG-agarose affinity columns (resin from Sigma-Aldrich); isotype-matched rat control antibodies (IgG1) and anti-CD11b (clone OX 42) were obtained from BD Pharmingen (Heidelberg, Germany); fractionated human IgG with irrelevant specificity and FITC-conjugated goat anti-rat secondary antibody from Sigma-Aldrich; anti-macrophage BM8 antibody, recognizing the F4/80 maturation antigen, from Dianova (Hannover, Germany); and Alexa Fluor® 568 conjugated goat anti-rat secondary antibody from Molecular Probes (Invitrogen, Karlsruhe, Germany).

2.2. Cell lines

Hybridoma cell line MK271 was from ATCC, Manassas, VA, USA; hybridoma cell line 390 was from S. Albelda, University of Pennsylvania, Philadelphia, PA, USA; hybridoma cell line Meca32 was from E. Butcher, Stanford University, Stanford, CA, USA. Murine brain endothelioma cells bEnd.3 were obtained from B. Engelhardt, Theodor Kocher Institute, University of Bern, Switzerland. A2780 is a human ovarian cancer cell line obtained from M. Wiese, Pharmac. Dept., University Bonn. Human tumor cell line Colo677, originally described as non-small cell lung cancer cell line, is a myeloma cell line from DSMZ, Braunschweig, Germany, which forms solid tumors with VCAM-positive vessels after subcutaneous injection [38]. All cell lines except bEnd.3 were cultured in RPMI 1640 medium supplemented with 10% foetal calf serum (FCS), 100 U penicillin and 100 μg streptomycin at 37 °C in a 5% CO_2 incubator. The bEnd.3 cells were grown in Dulbecco's modified Eagle's medium (DMEM) supplemented with 10% FCS, 100 U penicillin, 100 μg streptomycin and 4 mM glutamine. All cell culture reagents were obtained from Sigma-Aldrich.

2.3. Liposome preparation and characterisation

Liposomes were prepared from soyPC/Cholesterol/cyanur-PEG$_{2000}$-PE/DiO in a ratio of 64.5/30/5/0.5 mol%. In some preparations, trace amounts of [^{3}H]-cholesteryloleylether (Amersham, Buckinghamshire, U.K.) (0.25 μCi/μmol lipid) or 0.1 mol% rhodamine-DSPE (Avanti Polar lipids, Alabaster, USA) was added instead of the DiO label. Lipid films were hydrated with a 0.9% NaCl solution to reach a final lipid concentration of 30 mM. Unilamellar liposomes were prepared with a Mini-extruder, (Avanti Polar Lipids, Alabaster, USA),

from multilamellar vesicles extruded 19 times through a 200 nm polycarbonate membrane, 19 times through a 100 nm polycarbonate membrane and 10 times through a 50 nm polycarbonate membrane (Whatman Nuclepore 18 mm polycarbonate membrane, Richmond, USA). To couple a protein to the liposomal surface, the cyanur-PEG$_{2000}$-PE anchor was used, which couples the targeting devices to the terminal ends of the PEG chain [42]. An anti-VCAM monoclonal antibody (mAb) (M/K-271) was used as a homing device. Control liposomes were coupled to an irrelevant IgG (human fractionated IgG with ~70% IgG1 content or purified rat IgG1) or to bovine serum albumin (BSA) (grade V). Coupling was performed in a 1:1000 protein:lipid molar ratio. The cyanur ILs were prepared as previously described [12]. Briefly, the calculated amount of antibody was added to liposomes in borate buffer (pH=8.8) and incubated at room temperature for about 16 h. Unbound antibodies were separated by gel permeation chromatography using a Sepharose 4B column.

Liposomes were characterised with respect to particle size by dynamic light scattering (Malvern autosizer IIc, Malvern, UK), and with regards to phospholipid concentration [43]. The concentration of coupled proteins was determined with a modified Lowry assay [44]. Briefly, the proteins were first precipitated with 0.3% Na-deoxycholate and 70% trichloric acid and centrifuged for 20 min at 11,000 rpm at 4 °C. Thereafter, 1 ml of buffered CuSO$_4$ solution C was added (2 mM CuSO$_4$ * 5H$_2$O, 3.3 mM Na$_3$C$_6$H$_5$O$_7$ * 2H$_2$O, 3.8 mM Na$_2$CO$_3$, 2 mM NaOH), vortexed, and incubated at room temperature for 10 min. 50 μl Folin–Ciocalteus phenol was added and the samples were vortexed and incubated for 30 min at room temperature in the dark. Absorbance was read at A$_{750}$. A calibration curve was performed using either human IgG or BSA as reference for the respective liposomes.

2.4. Fluorescence associated cell sorting (FACS) analysis

VCAM-1 expression on activated bEnd.3 cells was analysed by FACS. bEnd.3 cells were incubated with 50 ng/ml TNF-α for 4 h, detached with 0.025% EDTA, rinsed twice in washing buffer (PBS containing 1% BSA) and fixed in 4% neutral buffered paraformaldehyde for 10 min at room temperature. After two more washes, cells were stained with rat anti-mouse VCAM mAb MK271 (10 μg/ml) for 1 h on ice and labelled with FITC-conjugated goat anti-rat secondary antibody for 30 min on ice, prior to analysis on a flow cytometer (BD Biosciences, San Jose, CA, USA).

Liposomal binding to the b.End3 cells was determined by FACS analysis. bEnd.3 cells were seeded in 96-well microtiter plates (density: 1×10^5 cells/well) 24 h prior to the assay. The cells were activated with TNF-α (50 ng/ml) for 4 h to ensure VCAM expression. Four different liposome preparations carrying a DiO label, were investigated: anti-VCAM mAb-liposomes (α-VCAM-L), liposomes conjugated to rat IgG1 (rIgG-L) or human IgG (hIgG-L) of irrelevant specificity and albumin-liposomes (Alb-L). The liposomes (75 nmol) were incubated with the cells for 1 h at 4 °C in normal cell medium. Unbound liposomes were removed by washing with PBS. The cells were detached with 0.025% EDTA and liposomal binding was analysed on the flow cytometer.

2.5. Fluorescence based cell assay

Binding of VCAM-directed liposomes to murine endothelial cells was also measured using a fluorescence based cell assay in comparison to control liposomes. Murine endothelial cells bEnd.3 were seeded and activated with TNF-α as described in Section 2.4.

Four different liposome preparations (see Section 2.4) carrying a DiO label, were investigated. The liposomes (75 nmol) were incubated with the cells for 1 h at 4 °C in normal cell medium. Unbound liposomes were removed by washing with PBS containing 1 mM CaCl$_2$ and 0.5 mM MgCl$_2$ and the liposomal binding was analysed in a FLUOstar Optima microplate reader (BMG Labtech, Offenburg, Germany).

To measure internalisation of VCAM-directed liposomes upon binding to bEnd.3 endothelial cells, the same procedure was followed as described above except that the cells were incubated with liposomes for 2 h at 37 °C. Thereafter, unbound liposomes were removed by washing with PBS containing 1 mM CaCl$_2$ and 0.5 mM MgCl$_2$ and liposome binding was measured. To determine the fraction of cell-associated liposomes that were internalised, the cells were stripped of their surface-bound liposomes by one wash with citrate buffer (pH=3.0) followed by one wash with PBS. The remaining cell-associated liposomes were considered internalised.

2.6. Dynamic flow assay

In order to simulate the *in vivo* binding of the liposomes to the endothelial cells under shear force conditions, a dynamic flow assay was performed as previously described [17]. Briefly, the endothelial cells were seeded on circular (18 mm) coverslips (5×10^5 cells) 24 h prior to the assay. The cells were activated with TNF-α (50 ng/ml) for 4 h and subsequently washed once with PBS. The coverslips were inserted into a doublet flow chamber. Each chamber was perfused with 5 ml of RPMI 1640 medium containing 1% penicillin/streptomycin, 10% FCS and 0.5 μmol liposome dispersion for 20 h at a shear rate mimicking capillary blood flow (about 200 s^{-1}) using a peristaltic pump at a temperature of approx. 37 °C. Two different liposome preparations, carrying a rhodamine label, were investigated; α-VCAM-L and hIgG-L. At different time points ($t=0$, 1 h, 2 h and 20 h), the flow was stopped and pictures of the liposomal binding to the cell layer were taken through an inverted fluorescence microscope Axiovert 200 equipped with a AxioCam MRc camera (Carl Zeiss, Germany).

2.7. Xenograft mouse model and biodistribution studies

Female CD1 nude mice (Charles River Laboratories, Germany) were housed in cages with free access to food and water with a 12 h light/dark cycle. Human Colo 677 xenograft tumors were created by a subcutaneous co-injection of 1×10^7 Colo 677 cells with Matrigel (BD Science, Heidelberg, Germany) diluted 1:1 into one flank of 4–5 week-old mice. The tumor size was measured every second day with a calliper in three perpendicular directions a, b and c, and tumor volumes were calculated according to the formula $V = \pi/6 \times a \times b \times c$. When the tumors had grown to 200–500 mm^3, the mice were injected with 0.5 μmol liposomes into the tail vein. Three different liposome preparations were investigated; α-VCAM-Ls, irrelevant IgG-liposomes and albumin-liposomes ($n=3$ per group), all containing DiO as a fluorescent label. The mice were sacrificed either 30 min or 24 h after liposome injection. Experiments were terminated by transcardial perfusion of deeply anesthetised mice with PBS for 10 min and major organs and tumors were snap frozen in dry ice/isopentane slush and stored at −80 °C until further use. The organs and tumors were cut into 5 μm sections on a Leica CM 3050 G cryostat (Leica, Wetzlar, Germany) and were either used directly or stored at −80 °C.

Total liposome tumor accumulation and biodistribution was investigated using Tritium-labelled liposomes. [^{3}H]-labelled liposomes coupled to either anti-VCAM antibody or an irrelevant human IgG were injected i.v. at a dose of 0.5 μmol liposome/mouse ($n=4$–5 mice per group). The animals were anesthetised after 24 h and blood was collected by heart puncture. This was followed by a transcardial perfusion with PBS for 10 min before liver, spleen, kidney, lungs, heart, skin, muscle and tumor were removed, weighed and stored at −20 °C until further use. To measure the amount of accumulated radioactive liposomes in the organs and tumor, the tissues were homogenised using a Potter Elvehjelm tube in 3 ml homogenisation buffer (50 mM Tris–HCl; 100 mM NaCl, 1 mM EGTA, 10 mM MgCl$_2$, 1% Triton X-100) per gram of tissue. Radioactivity was measured in 500 μl tissue homogenate after adding 100 μl of 10% SDS and 4 ml scintillation liquid (Ultima Gold). Blood samples were allowed to clot for 3 h and centrifuged for 20 min at 13,520 ×g at 4 °C [12].

2.8. Fluorescence microscopy of tissue sections

Cryosections of tumors and organs from the mouse tumor model were thawed, fixed in 4% paraformaldehyde for 10 min and incubated with one of the following primary antibodies: rat anti-mouse CD31 or rat anti-mouse Meca32 against endothelial cells; rat anti-mouse BM8 against macrophages; and rat anti-mouse CD11b against macrophages and dendritic cells. Sections were incubated with primary antibodies for 1 h at room temperature. Excess primary antibody was removed by three successive washes for 5 min with PBS. Thereafter, Alexa Fluor 568 conjugated secondary antibody was applied for 1 h at room temperature, followed by three washes with PBS. Coverslips were mounted with a fluorescence-mounting medium (Dako, Glostrup, Denmark). The sections were stored in the dark at 4 °C until further analysis. Overlay analysis was performed using AxioVision software (Carl Zeiss AxioVision release 4.6). Percentages of liposomes co-localised with the endothelium were determined in four randomised microscopic fields and calculated as the ratio between the amount of co-localised pixels×100 and the number of total green pixels. The co-localisation percentages are given as mean±SD.
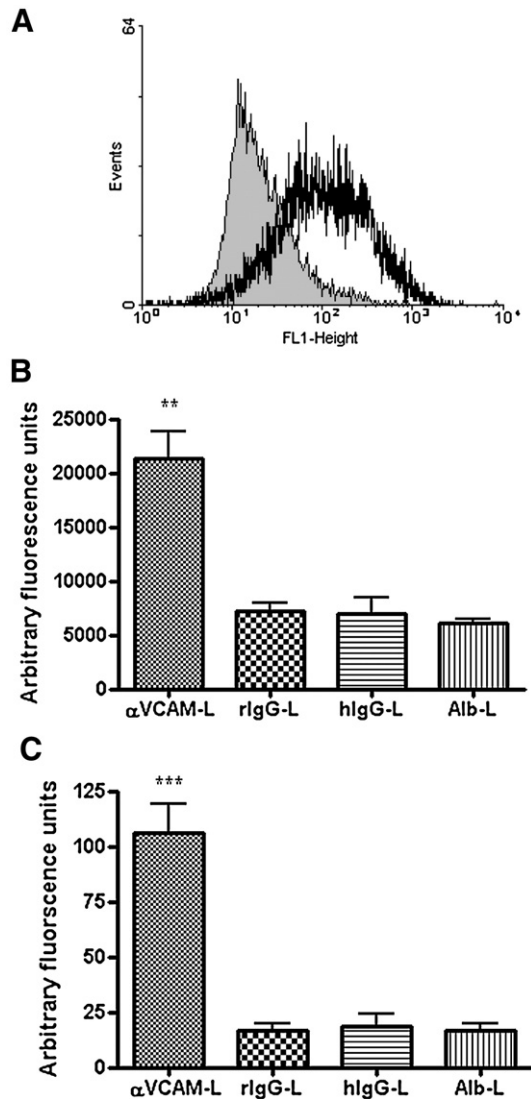
Fig. 1. The *in vitro* targeting of liposomes to VCAM-1 expressing bEnd.3 cells A: FACS analysis of the increased VCAM-1 expression of bEnd.3 cells after activation with TNF-α (50 ng/ml) for 4 h. The grey peak illustrates the non-activated cells; the black line illustrates the TNF-α activated cells. B: Comparison of the binding efficiency of anti-VCAM directed ILs (α-VCAM-L), ILs with coupled rat IgG1 (rIgG-L) or human IgG (hIgG-L) of irrelevant specificity and albumin (Alb-L) to bEnd.3 cells using the fluorescence based cell assay, **p<0.005 α-VCAM-L versus all three control liposome populations. C: Comparison of the targetability of α-VCAM-L, rIgG-L, hIgG-L and Alb-L to activated bEnd.3 cells analysed by FACS. ***p=0.001 α-VCAM-L versus all control liposomes. Data points represent the average of at least three experiments, error bars are SD.

2.9. Statistical analysis

Statistical significance between groups in the *in vitro* binding assays and in the *in vivo* biodistribution experiment was calculated using unpaired Student's *t*-test. Significance was assumed at a *p*-value<0.05.

3. Results and discussion

3.1. Targeting of VCAM-directed ILs to bEnd.3 cells in vitro

The murine endothelial cell line bEnd.3 was chosen for the establishment of an *in vitro* model of vascular liposomal targeting. Flow cytometry was used to ensure that these cells

indeed expressed VCAM-1 on their surface. Although the non-activated bEnd.3 cells also exhibited some surface expression of VCAM, 4 h incubation with TNF-α increased VCAM expression, as illustrated in Fig. 1A. Based on these data, all further experiments were carried out with bEnd.3 cells activated for 4 h with TNF-α.

Fluorescence-labelled liposomes were prepared with different proteins coupled to the PEG terminus via cyanur-PEG$_{2000}$-PE anchor. Liposomes carrying anti-VCAM mAb (α-VCAM-L) were compared to liposomes carrying a rat IgG1 (rIgG-L) or a human IgG of irrelevant specificity (hIgG-L) and albumin-conjugated liposomes (Alb-L). The liposomes were characterised with respect to particle size and coupling efficiency, as illustrated in Table 1.

The liposome populations were comparable in size and protein coupling, therefore, any differences in targeting behaviour should not be related to their physical characteristics. Furthermore, protein coupling did not significantly influence the liposomal size distribution. Size characteristics were constant and remained unchanged throughout the experiments.

The targetability of the four different liposomal preparations to activated bEnd.3 cells was initially analysed in a fluorescence microplate assay. α-VCAM-L bound with significantly higher intensity (p<0.005) to the activated endothelial cells than control liposomes, as illustrated in Fig. 1B. There were no differences between binding of the purified rat IgG1-conjugated liposomes (rIgG-L) and the fractionated human IgG-conjugated liposomes (hIgG-L) to the target cells. Furthermore, no binding to a VCAM-negative control cell line (A2780, data not shown) was observed.

Binding was also analysed by flow cytometry, since the interrogation of single cells in solution represents more accurate data and generally gives better signal to background ratios by eliminating background fluorescence remaining in the well after washes. Indeed, the VCAM-mediated binding of α-VCAM-L was not only confirmed but showed a higher difference in comparison with negative controls (Fig. 1 C; p<0.001). Static binding of liposomes to the cell surface does not mimic the vascular targeting of liposomes under physiological shear force conditions in circulation, especially considering the highly variable flow conditions in tumor vasculature [45]. Therefore, we employed a flow chamber assay [17] to investigate whether liposome binding was sufficient to target bEnd.3 cells under shear force conditions similar to those found in capillary venules. Binding of α-VCAM-L and hIgG-L to endothelial cells was followed microscopically over a time period of 20 h. As shown

Table 1
Comparison of the liposomal characteristics with respect to particle size and protein coupling yield

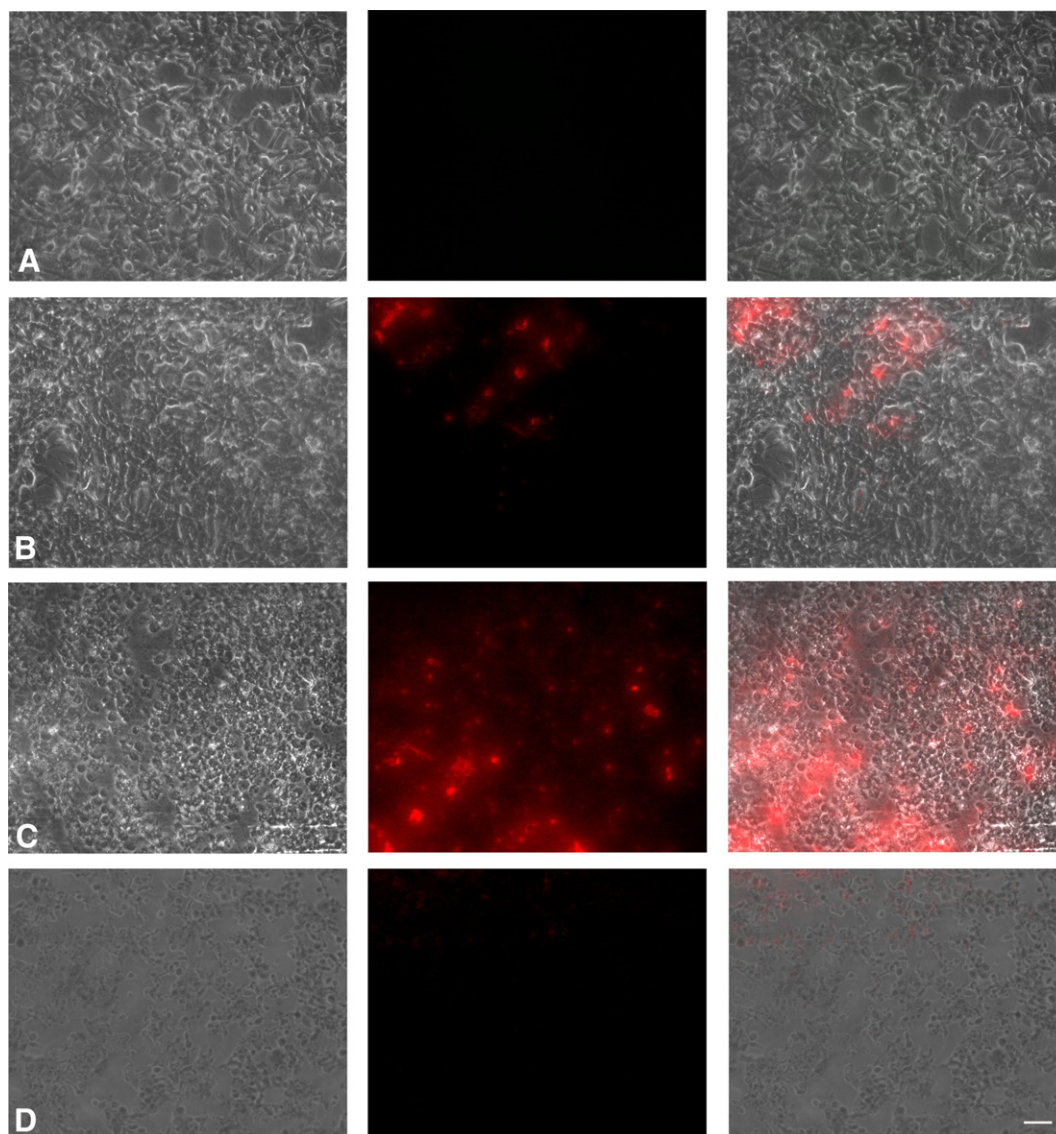|	Particle size(nm)	Polydispersity	μg protein/ μmol PL	Protein content: molecule per liposome
α-VCAM-L	83.1±14.4	0.13±0.05	59.0±17.9	52.3±15.8
rIgG-L	93.4±12.0	0.15±0.04	67.0±51.8	68.2±36.1
hIgG-L	91.3±13.2	0.12±0.06	74.4±40.2	71.1±35.2
Alb-L	84.5±13.1	0.15±0.06	70.3±42.0	85.0±4.31

Fig. 2. Binding of rhodamine-labelled α-VCAM-L to stimulated bEnd.3 cells under shear force conditions, illustrated as a phase contrast image (left), as fluorescence image (middle) and as an overlay image (right). The binding of rhodamine-labelled α-VCAM-L onto the cell monolayer was analysed at 0, 1 and 20 h (A–C) and compared to the binding of rhodamine-labelled hIgG-L after 20 h (D). The bar represents 50 μm.

in Fig. 2 A–C, the binding of α-VCAM-L to the cell layer increased in a sustainable manner illustrated by the increasing fluorescence intensity with time. In contrast, no binding was observed with the hIgG-L (Fig. 2 D).

It has previously been shown that VCAM-targeted liposomes were internalised upon binding [19]. We investigated the endocytosis of VCAM-targeted liposomes and found that approximately 8% of the bound α-VCAM-L were internalised by the activated endothelial cells after 2 h at 37 °C; therefore the staining of the bEnd.3 cells (Fig. 2 C) represents both internalised and surface-bound liposomes.

3.2. Targeting of α-VCAM-liposomes to tumor endothelial cells in vivo

Since the *in vitro* results appeared promising, the vascular targeting of α-VCAM-L was investigated in mice bearing human Colo 677 xenograft tumors. In this model solid tumors are formed upon subcutaneous injection of tumor cells and $\sim 30\%$ of the tumor vasculature is VCAM-positive [38]. The
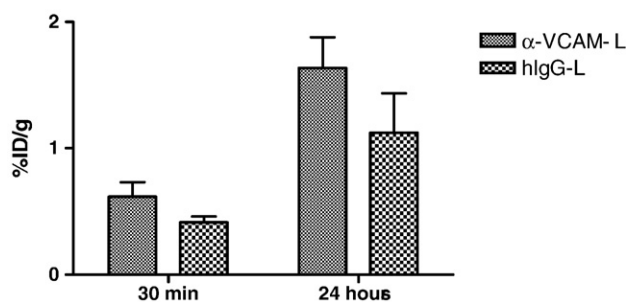

Fig. 3. Comparison of the quantitative tumor accumulation of α-VCAM-L and hIgG-L. The [^{3}H]-activity in tumors was detected 30 min and 24 h after injection of the [^{3}H]-labelled liposomes into Colo 677 tumor xenograft mice (data are mean±SD, $n \geq 4$).
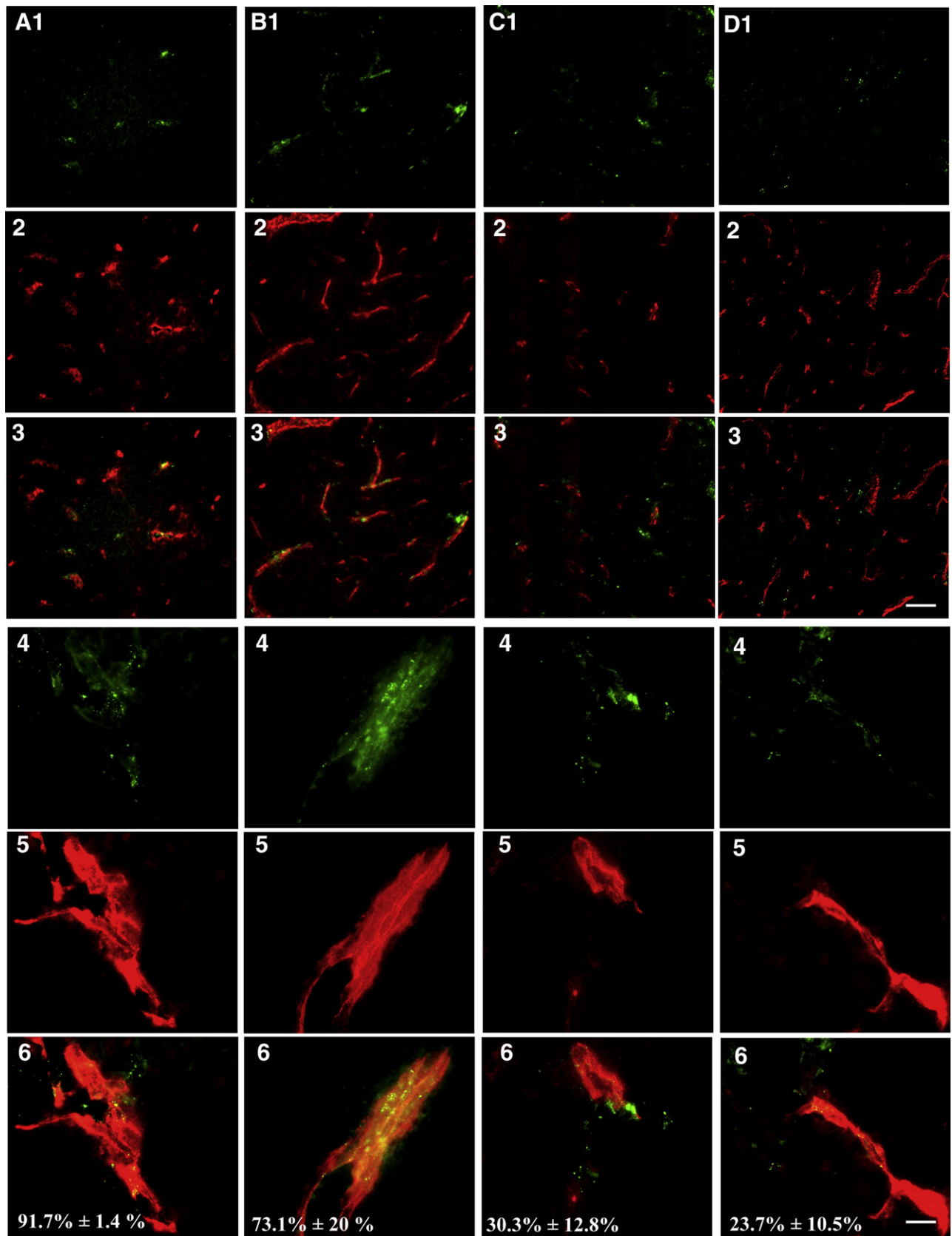
Fig. 4. Localisation of the different liposome populations within the tumors. (A1–6) α-VCAM-L 30 min after i.v. injection; (B1–6) α-VCAM-L 24 h after i.v. injection; (C1–6) hIgG-L 24 h after i.v. injection; (D1–6) Alb-L, 24 h after i.v. injection illustrating high degree of co-localisation for A and B, but not for C and D. 1) liposome distribution (green); 2) endothelial staining with CD31 (red); 3) overlay at low magnification; 4) liposome distribution (green); 5) endothelial staining with CD31 (red); and 6) overlay at high magnification of liposome distribution (green) and endothelial marker CD31 (red). The bar in the low magnification images corresponds to 50 μm. The bar in the high magnification images corresponds to 5 μm.

model was chosen because in mice, VCAM expression on tumor blood vessels in other tumor models is generally low, in contrast to tumor vascular VCAM expression in humans [38].

First, the tumor accumulation of α-VCAM-L versus hIgG-L, 30 min and 24 h after i.v. injection was quantified detecting the [^{3}H]-labelled liposomes in the tumor tissue. The data given in Fig. 3 indicates that the accumulation of both liposomal populations increased with time. At 24 h, about 2% of the injected dose per gram of tissue were localised to the tumor, although – in contrast to human tumors – only ~30% of tumor vessels show a medium strong expression of VCAM-1 in this mouse model [38].

The tumor accumulation of VCAM-directed ILs was slightly higher than that of control liposomes, but this difference did not reach statistical significance. This was not unexpected and should be related to unspecific tumor accumulation of the control liposomes. Unspecific accumulation of liposomes has been described previously [40,41,46] and is attributed to an enhanced permeability and retention effect [47]. However, differences between unspecific and specific tumor targeting of liposomes can not be distinguished by this quantitative evaluation.

In order to evaluate whether vascular-directed versus unspecific ILs were localised to different compartments within the tumor, we investigated the targeting behaviour of DiO-labelled ILs by fluorescence microscopy. The images, given in Fig. 4 clearly indicate that tumor accumulation of α-VCAM-L already was evident after 30 min (Fig. 4 A1) and had further increased by 24 h (Fig. 4 B1). At both time points the tumor accumulation of α-VCAM-L was more intense than that of both control liposomes (Fig. 4 C1–D1), which was not expected according to the data in Fig. 3. The lower fluorescence intensity of the control liposomes in the tumors could be related to a higher degree of extravasation and dilution of the liposomes throughout the tumor, so that their fluorescence is below the detection level.

To confirm whether the different liposomes were localised to tumor vasculature, tumor sections were counterstained with a fluorescent antibody against murine CD31 (Fig. 4 A2–D2). This double labelling procedure (Fig. 4 A3 and B3 low magnification, A6 and B6 high magnification) revealed a clear co-localisation between the α-VCAM-L and the endothelium after 30 min (91.7%) and after 24 h (73.1%). On the contrary, both types of control liposomes displayed a much lower degree of co-localisation with vascular endothelium (30.3% and 23.7%, resp.; Fig. 4 C3–D3 low magnification, C6–D6 high magnification). Endothelial cells are known to express receptors both for the Fc portion of antibodies [48] and for albumin [49]. Labelling of activated endothelial cells with a negative control IgG-antibody coupled to nanoparticles has been described in a mouse model for vascular inflammation [50]. This background binding could probably be decreased if recombinant antibody fragments devoid of the Fc portion, such as single chain variable fragments, were to be used as a targeting moiety.

Our data indicate that the α-VCAM-L behaves differently from the unspecific tumor accumulation of non-targeted liposomes arguing for a specific and receptor-mediated vascular targeting. Similar to this study, Kirpotin et al. recently investigated

Table 2
Biodistribution of α-VCAM-L and hIgG-L after 24 h as % injected dose per gram tissue

	Muscle	Skin	Heart	Lung	Kidney	Spleen	Liver	Blood
α-VCAM-L	0.25±	0.69±	1.03±	1.85±	3.59±	3.40±	8.11±	1.02±
24 h	0.18	0.45	0.67	0.94	2.14	2.32	1.24	0.82
hIgG-L	0.46±	0.99±	0.97±	1.66±	2.65±	3.3±	6.72±	1.11±
24 h	0.14	0.53	0.37	0.13	1.73	0.26	2.20	0.39
Statistics ($p=$) 24 h	0.131	0.42	0.893	0.747	0.546	0.945	0.286	0.864

the distribution and localisation of liposomes targeted against tumor cells as compared to non-targeted liposomes. Their results showed that although approximately the same amounts of liposomes were found in the tumor, the specific localisation of the liposomes differed. The non-targeted liposomes accumulated in the perivascular and extracellular space, whereas the targeted liposomes were found in the tumor cell cytosol [51]. Knowledge about the cellular distribution within the tumor is important for the choice of an appropriate effector molecule.

3.3. The localisation of liposomes in organs

To investigate whether α-VCAM-L would target vasculature outside the tumor, the localisation of the liposomes in major organs, such as heart, lung, liver, spleen and kidney, was investigated. The biodistribution of the liposomes was quantitatively determined using [^{3}H]-labelled α-VCAM-L and hIgG-L with subsequent activity detection in the organs after 24 h. The data given in Table 2 indicate that the majority of liposomes was detected in the liver (8% ID/g), followed by kidney, spleen, and lung, whereas other organs showed lower liposome accumulation. A high uptake into liver, spleen and lung was not unexpected, since localisation of liposomes into these organs is a well known phenomenon and is generally attributed to extraction via the RES [41]. No statistically significant differences were seen between VCAM-targeted liposomes and control liposomes, consistent with unspecific accumulation as part of the liposome elimination pathway. This is different from previous reports with both NGR-targeted and RGD-targeted liposomes, which accumulate in higher amounts in the lung and/or spleen [52,53].

To define the tissue compartments to which the liposomes localised, a similar study as described above was carried out. Cryostatic sections of lungs, kidneys, liver and spleen from mice injected with DiO-labelled liposomes (Fig. 5 A–D, left images) were counterstained with fluorescent antibodies detecting either endothelial cells (Fig. 5 A–D, middle) or tissue resident macrophages (Fig. 5 A–D, right). Liposome signals in the lung were rare and, if present, co-localised primarily with alveolar macrophages (Fig. 5 A, right). Fluorescent signals in the kidney were observed in glomeruli, occasionally on endothelial cells, in tubuli and as scattered events. Glomerular stain could be explained by VCAM expression of mesangial cells [36]. In contrast to human kidneys [34], endothelial cells in murine kidneys show a low level of VCAM expression [54] and
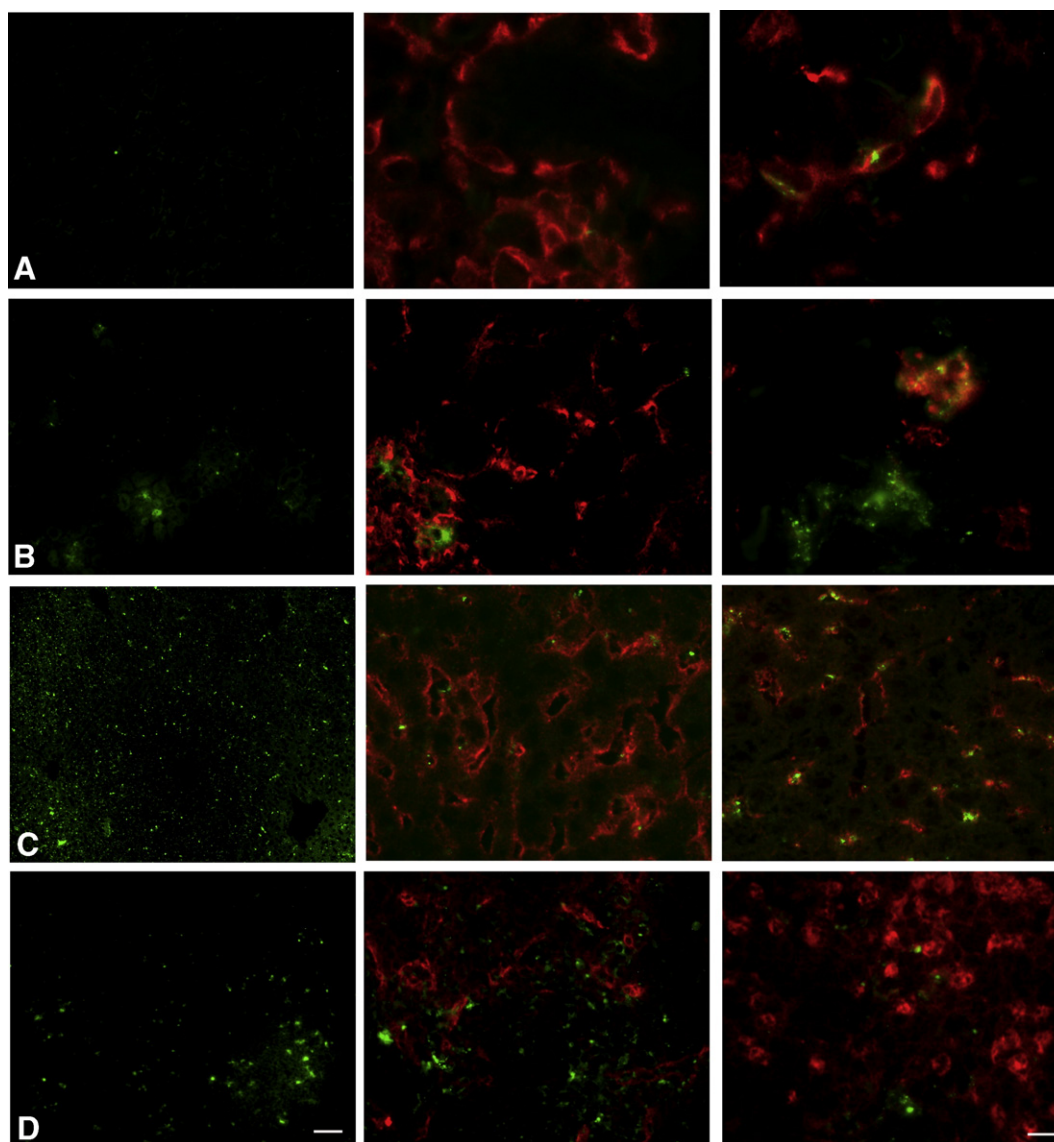
Fig. 5. Distribution of liposomes in lung, kidney, liver and spleen from tumor bearing mice 24 h after i.v. injection. A: Lung section showing the α-VCAM-L distribution (left); lung section double-stained against the endothelial marker Meca32 (middle); and double-stained against the macrophage marker CD11b (right). Note that the liposomes in the lung are co-localised with the lung macrophages. B: Kidney section showing the distribution of α-VCAM-L (left); kidney section double-stained against the endothelial marker CD31 (middle); and kidney section double-stained against the macrophage marker CD11b (right). C: Liver section illustrating the α-VCAM-L (green) distribution (left); liver section double-stained against the endothelial marker Meca32 (middle); and liver section double-stained against the macrophage marker F4/80 (right). Note the clear co-localisation between the liver macrophages and liposomes. D: Spleen section showing the distribution of VCAM-L (green) in the white pulp and marginal zone (left); spleen section double-stained against the endothelial marker Meca32 (middle); and spleen section double-stained against the macrophage and dendritic cell marker CD11b (right). The bar in the low magnification images corresponds to 50 μm. The bar in the high magnification images corresponds to 5 μm.

Gottstein C., unpublished data]. The tubular stain appeared more diffuse and might be due to free dye reabsorbed by the tubuli after escaping into the glomerular filtrate. Scattered staining was found within tubular lumina, and also in co-localisation with kidney macrophages (Fig. 5 B, right).

The liver sections exhibited a clear co-localisation between the liposomes and liver macrophages (Fig. 5 C, right image), while virtually no co-localisation was observed in sections stained against the endothelium (Fig. 5 C, middle).

In the spleen, liposome signals were prominent in the marginal zone, in accordance with previous studies [55,56]. No co-localisation with spleen vasculature was observed (Fig. 5 D,

middle). Instead, we found co-localisation with F4/80 positive macrophages in the red pulp (not shown) and with CD11b positive cells (Fig. 5 D, right). CD11b is a marker for macrophages and also for dendritic cells, which are known to express VCAM-1.

In summary, these results provide evidence, for the first time, that immunoliposomes can be effectively targeted to tumor vasculature *in vivo*. No significant vascular binding was observed to any of the organs investigated, although further studies are needed to evaluate localisation in a broader set of normal tissues. This recommends VCAM-1 targeted ILs as candidate drug carriers for tumor vascular delivery.

While VCAM-1 expression on vasculature is for the most part restricted to pathological conditions, several non-vascular cells also express VCAM-1 [35,36]. This is of minor concern as long as effectors are chosen, that are designed to alter vascular specific functions. Examples include angiogenesis inhibitors, sensitizers for specific vascular occlusion-inducing agents [57] and intracellularly acting modifiers of angiogenesis associated signal transduction pathways [58].

4. Conclusions

The tumor vasculature has been recognized as an attractive drug target, and the means for efficient delivery of payloads to tumor vascular markers are in demand. We have generated long circulating immunoliposomes (ILs) targeted to VCAM-1. This study provides the evidence that 1) α-VCAM-Ls specifically bound to activated endothelial cells *in vitro* under static and flow conditions; 2) α-VCAM-Ls, but not control liposomes, effectively targeted tumor endothelial cells *in vivo*; 3) localisation of VCAM-targeted ILs in non-target organs was primarily found in phagocytic cells and not co-localised to the vasculature and 4) RES uptake of the targeted ILs is not significantly higher compared to non-targeted ILs.

In summary, PEGylated α-VCAM-Ls are candidate drug carriers for delivery of vascular specific payloads to tumor vasculature and further studies are warranted to evaluate their suitability for clinical applications.

Acknowledgements

References

[1] D. Chaplin, M.R. Horsman, D.W. Siemann, Current development status of small-molecule vascular disrupting agents, Curr. Opin. Investig. Drugs 7 (2006) 522–528.
[2] P. Thorpe, Vascular targeting agents as cancer therapeutics, Clin. Cancer Res. 10 (2004) 415–427.
[3] J. Folkman, Angiogenesis, Ann. Rev. Med. 57 (2006) 1–18.
[4] T. Boehm, J. Folkman, T. Browder, M.S. O'Reilly, Antiangiogenic therapy of experimental cancer does not induce acquired drug resistance, Nature 390 (1997) 404–407.
[5] F.J. Burrows, P.E. Thorpe, Vascular targeting — a new approach to the therapy of solid tumors, Pharmacol. Ther. 64 (1994) 155–174.
[6] J. Folkman, The role of angiogenesis in tumor growth, Semin. Cancer Biol. 3 (1992) 65–71.
[7] T.M. Allen, The use of glycolipids and hydrophilic polymers in avoiding rapid uptake of liposomes by the mononuclear phagocyte system, Adv. Drug Deliv. Rev. 13 (1994) 285–309.
[8] R. Kontermann, Immunoliposomes for cancer therapy, Curr. Opin. Mol. Ther. 8 (2006) 39–45.
[9] C. Hansen, G.Y. Kao, E.H. Moase, S. Zalipsky, T.M. Allen, Attachment of antibodies to sterically stabilized liposomes: evaluation, comparison and optimization of coupling procedures, BBA 1239 (1995) 133–144.
[10] T. Allen, E. Brandeis, C. Hansen, G. Kao, S. Zalipsky, A new strategy for attachment of antibodies to sterically stabilized liposomes resulting in efficient targeting to cancer cells, BBA 1237 (1995) 99–108.
[11] J.A. Harding, C.M. Engbers, M.S. Newman, N.I. Goldstein, S. Zalipsky, Immunogenicity and pharmacokinetic attributes of poly(ethylene glycol)-grafted immunoliposomes, BBA 1327 (1997) 181–192.
[12] G. Bendas, U. Rothe, G.L. Scherphof, J.A.A.M. Kamps, The influence of repeated injections on pharmacokinetics and biodistribution of different types of sterically stabilized immunoliposomes, BBA 1609 (2003) 63–70.
[13] T. Volkel, P. Holig, T. Merdan, R. Muller, R.E. Kontermann, Targeting of immunoliposomes to endothelial cells using a single-chain Fv fragment directed against human endoglin (CD105), BBA 1663 (2004) 158–166.
[14] P. Benzinger, G. Martiny-Baron, P. Reusch, G. Siemeister, J.T. Kley, D. Marme, C. Unger, U. Massing, Targeting of endothelial KDR receptors with 3G2 immunoliposomes in vitro, BBA 1466 (2000) 71–78.
[15] P.G.M. Bloemen, P.A.J. Henricks, L. van Bloois, M.C. van den Tweel, A.C. Bloem, F.P. Nijkamp, D.J.A. Crommelin, G. Storm, Adhesion molecules: a new target for immunoliposome-mediated drug delivery, FEBS Lett. 357 (1995) 140–144.
[16] D.D. Spragg, D.R. Alford, R. Greferath, C.E. Larsen, K.-D. Lee, G.C. Gurtner, M.I. Cybulsky, P.F. Tosi, C. Nicolau, M.A. Gimbrone Jr., Immunotargeting of liposomes to activated vascular endothelial cells: a strategy for site-selective delivery in the cardiovascular system, PNAS 94 (1997) 8795–8800.
[17] S. Kessner, A. Krause, U. Rothe, G. Bendas, Investigation of the cellular uptake of E-selectin-targeted immunoliposomes by activated human endothelial cells, BBA 1514 (2001) 177–190.
[18] G.N.C. Chiu, M.B. Bally, L.D. Mayer, Targeting of antibody conjugated, phosphatidylserine-containing liposomes to vascular cell adhesion molecule 1 for controlled thrombogenesis, BBA 1613 (2003) 115–121.
[19] M. Voinea, I. Manduteanu, E. Dragomir, M. Capraru, M. Simionescu, Immunoliposomes directed toward VCAM-1 interact specifically with activated endothelial cells—a potential tool for specific drug delivery, Pharm. Res. 22 (2005) 1906–1917.
[20] S. Gosk, C. Gottstein, G. Bendas, Targeting of immunoliposomes to endothelial cells expressing VCAM: a future strategy in cancer therapy, Int. J. Clin. Pharmacol. Ther. 43 (2005) 581–582.
[21] M. Everts, G.A. Koning, R.J. Kok, S.A. Asgeirsdottir, D. Vestweber, D.K. Meijer, G. Storm, G. Molema, In vitro cellular handling and in vivo targeting of E-selectin-directed immunoconjugates and immunoliposomes used for drug delivery to inflamed endothelium, Pharm. Res. 20 (2003) 64–72.
[22] R.C. Scott, B. Wang, R. Nallamothu, C.B. Pattillo, G. Perez-Liz, A. Issekutz, L.D. Valle, G.C. Wood, M.F. Kiani, Targeted delivery of antibody conjugated liposomal drug carriers to rat myocardial infarction, Biotechnol. Bioeng. 96 (2007) 795–802.
[23] K. Temming, R.M. Schiffelers, G. Molema, R.J. Kok, RGD-based strategies for selective delivery of therapeutics and imaging agents to the tumour vasculature, Drug Resist. Updat. 8 (2005) 381–402.
[24] F. Pastorino, C. Brignole, D. Di Paolo, B. Nico, A. Pezzolo, D. Marimpietri, G. Pagnan, F. Piccardi, M. Cilli, R. Longhi, D. Ribatti, A. Corti, T.M. Allen, M. Ponzoni, Targeting liposomal chemotherapy via both tumor cell-specific and tumor vasculature-specific ligands potentiates therapeutic efficacy, Cancer Res. 66 (2006) 10073–10082.
[25] D. Simberg, T. Duza, J.H. Park, M. Essler, J. Pilch, L. Zhang, A.M. Derfus, M. Yang, R.M. Hoffman, S. Bhatia, M.J. Sailor, E. Ruoslahti, Biomimetic amplification of nanoparticle homing to tumors, PNAS 104 (2007) 932–936.
[26] M. Kondo, T. Asai, Y. Katanasaka, Y. Sadzuka, H. Tsukada, K. Ogino, T. Taki, K. Baba, N. Oku, Anti-neovascular therapy by liposomal drug targeted to membrane type-1 matrix metalloproteinase, Int. J. Cancer 108 (2004) 301–306.
[27] G.P. Adams, R. Schier, A.M. McCall, H.H. Simmons, E.M. Horak, R.K. Alpaugh, J.D. Marks, L.M. Weiner, High affinity restricts the localization and tumor penetration of single-chain Fv antibody molecules, Cancer Res. 61 (2001) 4750–4755.
[28] Y. Zhou, D.C. Drummond, H. Zou, M.E. Hayes, G.P. Adams, D.B. Kirpotin, J.D. Marks, Impact of single-chain Fv antibody fragment affinity

on nanoparticle targeting of epidermal growth factor receptor-expressing tumor cells, J. Mol. Biol. 371 (2007) 934–947.

[29] L. Osborn, C. Hession, R. Tizard, C. Vassallo, S. Luhowskyj, G. Chi-Rosso, R. Lobb, Direct expression cloning of vascular cell adhesion molecule 1, a cytokine-induced endothelial protein that binds to lymphocytes, Cell 59 (1989) 1203–1211.

[30] G.E. Rice, J.M. Munro, M.P. Bevilacqua, Inducible cell adhesion molecule 110 (INCAM-110) is an endothelial receptor for lymphocytes. A CD11/CD18-independent adhesion mechanism, J. Exp. Med. 171 (1990) 1369–1374.

[31] B. Garmy-Susini, H. Jin, Y. Zhu, R.-J. Sung, R. Hwang, J. Varner, Integrin $\alpha4\beta1$-VCAM-1-mediated adhesion between endothelial and mural cells is required for blood vessel maturation, J. Clin. Invest. 115 (2005) 1542–1551.

[32] H. Jin, J. Su, B. Garmy-Susini, J. Kleeman, J. Varner, Integrin {alpha}4 {beta}1 promotes monocyte trafficking and angiogenesis in tumors, Cancer Res. 66 (2006) 2146–2152.

[33] M. Klemke, T. Weschenfelder, M.H. Konstandin, Y. Samstag, High affinity interaction of integrin alpha4beta1 (VLA-4) and vascular cell adhesion molecule 1 (VCAM-1) enhances migration of human melanoma cells across activated endothelial cell layers, J. Cell. Physiol. 212 (2007) 368–374.

[34] I. Kuzu, R. Bicknell, C. Fletcher, K. Gatter, Expression of adhesion molecules on the endothelium of normal tissue vessels and vascular tumors, Lab. Invest. 69 (1993) 322–328.

[35] D. Ryan, B. Nuccie, C. Abboud, J. Winslow, Vascular cell adhesion molecule-1 and the integrin VLA-4 mediate adhesion of human B cell precursors to cultured bone marrow adherent cells, J. Clin. Invest. 88 (1991) 995–1004.

[36] D. Seron, J. Cameron, D. Haskard, Expression of VCAM-1 in the normal and diseased kidney, Nephrol. Dial. Transplant. 6 (1991) 917–922.

[37] R.L. Dedrick, S. Bodary, M.R. Garovoy, Adhesion molecules as therapeutic targets for autoimmune diseases and transplant rejection, Exp. Opin. Biol. Ther. 3 (2003) 85–95.

[38] A. Dienst, A. Grunow, M. Unruh, B. Rabausch, J.E. Nor, J.W. Fries, C. Gottstein, Specific occlusion of murine and human tumor vasculature by VCAM-1-targeted recombinant fusion proteins, J. Natl. Cancer Inst. 97 (2005) 733–747.

[39] I. Ricard, M. Payet, G. Dupuis, VCAM-1 is internalized by a clathrin-related pathway in human endothelial cells but its alpha 4 beta 1 integrin counter-receptor remains associated with the plasma membrane in human T lymphocytes, Eur. J. Immunol. 28 (1998) 1708–1718.

[40] S.K. Huang, K.D. Lee, K. Hong, D.S. Friend, D. Papahadjopoulos, Microscopic localization of sterically stabilized liposomes in colon carcinoma-bearing mice, Cancer Res. 52 (1992) 5135–5143.

[41] N. Emanuel, E. Kedar, E. Bolotin, N. Smorodinsky, Y. Barenholz, Targeted delivery of doxorubicin via sterically stabilized immunoliposomes: pharmacokinetics and biodistribution in tumor-bearing mice, Pharm. Res. 13 (1996) 861–868.

[42] G. Bendas, A. Krause, U. Bakowsky, J. Vogel, U. Rothe, Targetability of novel immunoliposomes prepared by a new antibody conjugation technique, Int. J. Pharm. 181 (1999) 79–93.

[43] B. Ames, D. Dubin, The role of polyamines in the neutralization of bacteriophage deoxyribonucleic acid, J. Biol. Chem. 235 (1960) 769–775.

[44] G. Peterson, A simplification of the protein assay method of Lowry et al. which is generally more applicable, Anal. Biochem. 83 (1977) 346–356.

[45] J. Denekamp, A. Dasu, A. Waites, Vasculature and microenvironmental gradients: the missing links in novel approaches to cancer therapy? Advan. Enzyme Regul. 38 (1998) 281–299.

[46] G.J.R. Charrois, T.M. Allen, Multiple injections of pegylated liposomal doxorubicin: pharmacokinetics and therapeutic activity, J. Pharmacol. Exp. Ther. 306 (2003) 1058–1067.

[47] Y. Noguchi, J. Wu, R. Duncan, J. Strohalm, K. Ulbrich, T. Akaike, H. Maeda, Early phase tumor accumulation of macromolecules: a great difference in clearance rate between tumor and normal tissues, Jpn. J. Cancer Res. 89 (1998) 307–314.

[48] T. Olafsen, V.E. Kenanova, A.M. Wu, Tunable pharmakokinetics: modifying the in vivo half-life of antibodies by directed mutagenesis of the Fc fragment, Nat. Protoc. 1 (2006) 2048–2060.

[49] F. Antohe, C. Heltianu, M. Simionescu, Albumin-binding proteins of endothelial cells: immunocytochemical detection of the 18 kDA peptide, Eur. J. Cell Biol. 56 (1991) 34–42.

[50] A. Tsourkas, V.R. Shinde-Patil, K.A. Kelly, P. Patel, A. Wolley, J.R. Allport, R. Weissleder, In vivo imaging of activated endothelium using an anti-VCAM-1 magnetooptical probe, Bioconj. Chem. 16 (2005) 576–581.

[51] D.B. Kirpotin, D.C. Drummond, Y. Shao, M.R. Shalaby, K. Hong, U.B. Nielsen, J.D. Marks, C.C. Benz, J.W. Park, Antibody targeting of long-circulating lipidic nanoparticles does not increase tumor localization but does increase internalization in animal models, Cancer Res. 66 (2006) 6732–6740.

[52] F. Pastorino, C. Brignole, D. Marimpietri, M. Cilli, C. Gambini, D. Ribatti, R. Longhi, T.M. Allen, A. Corti, M. Ponzoni, Vascular damage and anti-angiogenic effects of tumor vessel-targeted liposomal chemotherapy, Cancer Res. 63 (2003) 7400–7409.

[53] R.M. Schiffelers, G.A. Koning, T.L.M. ten Hagen, M.H.A.M. Fens, A.J. Schraa, A.P.C.A. Janssen, R.J. Kok, G. Molema, G. Storm, Anti-tumor efficacy of tumor vasculature-targeted liposomal doxorubicin, J. Control. Release 91 (2003) 115.

[54] J. Fries, A. Williams, R. Atkins, W. Newman, M. Lipscomb, T. Collins, Expression of VCAM-1 and E-selectin in an in vivo model of endothelial activation, Am. J. Pathol. 143 (1993) 725–737.

[55] D.C. Litzinger, A.M.J. Buiting, N. van Rooijen, L. Huang, Effect of liposome size on the circulation time and intraorgan distribution of amphipathic poly (ethylene glycol)-containing liposomes, BBA 1190 (1994) 99–107.

[56] P. Aichele, J. Zinke, L. Grode, R.A. Schwendener, S.H.E. Kaufmann, P. Seiler, Macrophages of the splenic marginal zone are essential for trapping of blood-borne particulate antigen but dispensable for induction of specific T cell responses, J. Immunol. 171 (2003) 1148–1155.

[57] J. Philipp, A. Dienst, M. Unruh, A. Wagener, A. Grunow, A. Engert, J.W. Fries, C. Gottstein, Soluble tissue factor induces coagulation on tumor endothelial cells in vivo if coadministered with low-dose lipopolysaccharides, Arterioscler. Thromb. Vasc. Biol. 23 (2003) 905–910.

[58] J.D. Hood, M. Bednarski, R. Frausto, S. Guccione, R.A. Reisfeld, R. Xiang, D.A. Cheresh, Tumor regression by targeted gene delivery to the neovasculature, Science 296 (2002) 2404–2407.